Configuration-Specific Kinetic Theory Applied to an Ideal Binary Gas Mixture

Floyd L. Wiseman

Senior Scientist, ENSCO, Inc., 4849 North Wickham Road, Melbourne, Florida 32940

Received: April 24, 2006; In Final Form: August 10, 2006

This paper is the second in a two-part series dealing with the configuration-specific analyses for molecular collision events of hard, spherical molecules at thermal equilibrium. The first paper analyzed a single-component system, and the reader is referred to it for the fundamental concepts. In this paper, the expressions for the configuration-specific collision frequencies and the average line-of-centers collision angles and speeds are derived for an ideal binary gas mixture. The analyses show that the average line-of-centers quantities are all dependent upon the ratio of the masses of the two components, but not upon molecular size. Of course, the configuration-specific collision frequencies do depend on molecular size. The expression for the overall binary collision frequency is a simple sum of the configuration-specific collision frequencies and is identical to the conventional expression.

Theory

Analysis of the Front- and Rear-End Collision Frequencies. The configuration-specific differential collision frequency, δZ_{AB}, between molecules of type A and those of type B is

$$\delta Z_{AB}(\alpha_A,\alpha_B,v_A,v_B) = \frac{\sigma_{AB} v_{lc}(\alpha_A,\alpha_B,v_A,v_B)\, P(\alpha_A,\alpha_B)\, \delta N_{v_A} \delta N_{v_B}}{V} \quad (1)$$

in which σ_{AB} is the collision cross-section, given by $\sigma_{AB} = \pi(r_A + r_B)^2$ (r_A and r_B are the molecular radii), $v_{lc}(\alpha_A,\alpha_B,v_A,v_B)$ is the line-of-centers speed, $P(\alpha_A,\alpha_B)$ is the angular probability distribution function, and δN_{v_i} is the number of i molecules (i is A or B) having speeds between v_i and $v_i + \delta v_i$. The independent variables α_A, α_B, v_A, and v_B are illustrated in Figure 1. The expression in eq 1 is identical to Kauzmann's;[1] the relative speed, however, has been replaced with the line-of-centers speed, which is given by[2]

$$v_{lc}(\alpha_A,\alpha_B,v_A,v_B) = v_A \cos\alpha_A - v_B \cos\alpha_B \quad (2)$$

in which α_i is the collision angle between the velocity vector, v_i, and the unit vector joining the centers of the two spherical molecules (see Figure 1). Note that all terms in eq 2 are scalar. The use of the line-of-centers speed rather than the relative speed in the analysis leads to configuration-specific parameters. The angular probability distribution function, which is defined as the probability that molecule A will collide at an angle between α_A and $\alpha_A + \delta\alpha_A$ and molecule B at an angle between α_B and $\alpha_B + \delta\alpha_B$, is given by

$$P(\alpha_A,\alpha_B) = \sin\alpha_A \sin\alpha_B\, \delta\alpha_A\, \delta\alpha_B \quad (3)$$

From kinetic molecular theory, δN_{v_i} is[3]

$$\delta N_{v_i} = \frac{4N_i}{\sqrt{\pi}} \beta_i^{3/2} v_i^2 e^{-\beta_i v_i^2}\, \delta v_i \quad (4)$$

in which $\beta_i = m_i/(2kT) = M_i/(2RT)$ (m_i is the mass of a single molecule, M_i is the molecular mass, k is Boltzmann's constant, and R is the gas constant.) Putting the explicit functions for $v_{lc}(\alpha_A,\alpha_B,v_A,v_B)$, $P(\alpha_A,\alpha_B)$, and δN_{v_i} into eq 1 yields

$$\delta Z_{AB}(\alpha_A,\alpha_B,v_A,v_B) = \frac{16 N_A N_B \sigma_{AB} (\beta_A\beta_B)^{3/2}}{\pi V} \sin\alpha_A \sin\alpha_B\, v_A^2 v_B^2 (v_A\cos\alpha_A - v_B\cos\alpha_B) e^{-\beta_A v_A^2} e^{-\beta_B v_B^2}\, \delta\alpha_A\, \delta\alpha_B\, \delta v_A\, \delta v_B \quad (5)$$

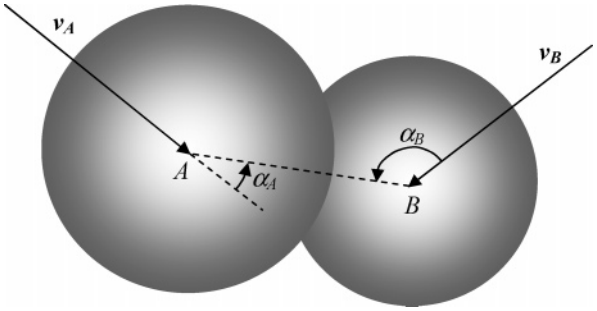

Figure 1. Representative configuration for a front-end collision between two nonidentical spherical molecules, A and B. The collision angles, α_A and α_B, are the angles between the velocity vectors, v_A and v_B, respectively, and the unit vector joining the centers of the two molecules.

For front-end collisions, α_A varies between 0 and $\pi/2$ and α_B between $\pi/2$ and π (this configuration is represented schematically as A → ← B), and the molecular speeds vary between 0 and ∞. Integrating eq 5 with these limits yields the following expression for the front-end collision frequency, $Z_{AB,front}$:

$$Z_{AB,front} = \int_0^\infty \int_0^\infty \int_{\pi/2}^{\pi} \int_0^{\pi/2} dZ_{AB}(\alpha_A,\alpha_B,v_A,v_B) = \frac{NPX_AX_B\sigma_{AB}\langle v_B\rangle(1+\rho)}{2kT} \quad (6)$$

in which $\rho = \sqrt{\beta_B/\beta_A} = \sqrt{m_B/m_A}$, X_A and X_B are the mole fractions, and $\langle v_B\rangle$ is the average molecular speed of B, given by $\langle v_B\rangle = \sqrt{8kT/(\pi m_B)}$.

10.1021/jp062497q CCC: $33.50
Published on Web 09/12/2006

For rear-end collisions, either α_A and α_B both vary between 0 and $\pi/2$ (represented as A → B →), or they both vary between $\pi/2$ and π (represented as ← A ← B). In the former case, v_A must fall within the range $v_B \cos \alpha_B/\cos \alpha_A \leq v_A \leq \infty$ to ensure that $v_{lc}(\alpha_A,\alpha_B,v_A,v_B) \geq 0$, and in the latter case, v_B must fall within the range $v_A \cos \alpha_A/\cos \alpha_B \leq v_B \leq \infty$ to ensure that $v_{lc}(\alpha_A,\alpha_B,v_A,v_B) \geq 0$. The collision frequencies for the first configuration, $Z_{A\rightarrow B,rear}$, and for the second, $Z_{A\leftarrow B,rear}$, are respectively[4]

$$Z_{A\rightarrow B,rear} = \int_0^{\infty}\int_{\gamma_A}^{\infty}\int_0^{\pi/2}\int_0^{\pi/2} dZ_{AB}(\alpha_A,\alpha_B,v_A,v_B) = \frac{NPX_AX_B\sigma_{AB}\langle v_B\rangle(\sqrt{1+\rho^2}-1)}{2kT} \quad (7)$$

$$Z_{A\leftarrow B,rear} = \int_{\gamma_B}^{\infty}\int_0^{\infty}\int_{\pi/2}^{\pi}\int_{\pi/2}^{\pi} dZ_{AB}(\alpha_A,\alpha_B,v_A,v_B) = \frac{NPX_AX_B\sigma_{AB}\langle v_B\rangle(\sqrt{1+\rho^2}-\rho)}{2kT} \quad (8)$$

in which $\gamma_A = v_B \cos \alpha_B/\cos \alpha_A$ and $\gamma_B = v_A \cos \alpha_A/\cos \alpha_B$. The overall rear-end collision frequency, $Z_{AB,rear}$, is simply the sum of $Z_{A\rightarrow B,rear}$ and $Z_{A\leftarrow B,rear}$:

$$Z_{AB,rear} = Z_{A\rightarrow B,rear} + Z_{A\leftarrow B,rear} = \frac{NPX_AX_B\sigma_{AB}\langle v_B\rangle(2\sqrt{1+\rho^2}-1-\rho)}{2kT} \quad (9)$$

Finally, the overall binary collision frequency is simply the sum of $Z_{AB,front}$ and $Z_{AB,rear}$:

$$Z_{AB} = Z_{AB,front} + Z_{AB,rear} = \frac{NPX_AX_B\sigma_{AB}\langle v_B\rangle\sqrt{1+\rho^2}}{kT} = \frac{NPX_AX_B\sigma_{AB}}{kT}\sqrt{\frac{8kT}{\pi\mu}} \quad (10)$$

in which μ is the reduced mass. Equation 10 is identical to the expression obtained by other investigators.[1,5,6]

The fraction of front-end collisions, η_{front}, is

$$\eta_{front} = \frac{Z_{AB,front}}{Z_{AB}} = \frac{1+\rho}{2\sqrt{1+\rho^2}} \quad (11)$$

The fraction of rear-end collisions in which A collides with B from behind, $\eta_{A\rightarrow B,rear}$, is

$$\eta_{A\rightarrow B,rear} = \frac{Z_{A\rightarrow B,rear}}{Z_{AB}} = \frac{\sqrt{1+\rho^2}-1}{2\sqrt{1+\rho^2}} \quad (12)$$

Finally, the fraction of rear-end collisions in which B collides with A from behind, $\eta_{A\leftarrow B,rear}$, is

$$\eta_{A\leftarrow B,rear} = \frac{Z_{A\leftarrow B,rear}}{Z_{AB}} = \frac{\sqrt{1+\rho^2}-\rho}{2\sqrt{1+\rho^2}} \quad (13)$$

Examining the expressions for $\rho = 0$, 1, and ∞ gives an idea of the range of possible values for the various configuration-specific parameters. Table 1shows values for the configuration-specific collision fractions for $\rho = 0$, 1, and ∞.[4] The limiting case where $\rho = 0$ represents a hypothetical system in which molecule A is infinitely massive and immobile. Conversely, the limiting case where $\rho = \infty$ represents a hypothetical system in which molecule B is infinitely massive and immobile. Except for these limiting cases, $\eta_{front} > \eta_{rear}$. Because the maximum value for η_{front} is somewhat less than 1, configuration-specific effects cannot be ignored for any gas-phase dynamic process for which front- and rear-end collision events exhibit distinctively different behavior.

TABLE 1: Values for the Configuration-Specific Collision Fractions for $\rho = 0$, 1, and ∞ ($\rho = \sqrt{m_B/m_A}$)

	$\rho = 0$	$\rho = 1$	$\rho = \infty$
η_{front}	$1/2$	$\frac{1}{\sqrt{2}}$ (~0.7071)	$1/2$
$\eta_{A\rightarrow B,rear}$	0	$\frac{1}{2}\left(1-\frac{1}{\sqrt{2}}\right)$ (~0.1464)	$1/2$
$\eta_{A\leftarrow B,rear}$	$1/2$	$\frac{1}{2}\left(1-\frac{1}{\sqrt{2}}\right)$ (~0.1464)	0

TABLE 2: Values for the Average Configuration-Specific Line-of-Centers Collision Angles for $\rho = 0$, 1, and ∞ ($\rho = \sqrt{m_B/m_A}$)

	$\rho = 0$	$\rho = 1$	$\rho = \infty$
$\langle\alpha_{A,front}\rangle$	1 (~57.30°)	$\frac{1}{2}\left(1+\frac{\pi}{4}\right)$ (~51.15°)	$\frac{\pi}{4}$ (45°)
$\langle\alpha_{B,front}\rangle$	$\frac{3\pi}{4}$ (135°)	$\frac{1}{2}\left(\frac{7\pi}{4}-1\right)$ (~128.85°)	$\pi - 1$ (~122.70°)
$\langle\alpha_{(A)\rightarrow B,rear}\rangle$	$2/3$ (~38.20°)	$\frac{1}{2}(\sqrt{2}+1)\left(\frac{\pi}{2}-1\right)$ (~39.48°)	$\frac{\pi}{4}$ (45°)
$\langle\alpha_{A\rightarrow(B),rear}\rangle$	$\frac{\pi}{2}$ (90°)	$\frac{\sqrt{2}+1}{2}$ (~69.16°)	1 (~57.30°)
$\langle\alpha_{(A)\leftarrow B,rear}\rangle$	$\pi - 1$ (~122.70°)	$\pi - \frac{\sqrt{2}+1}{2}$ (~110.84°)	$\frac{\pi}{2}$ (90°)
$\langle\alpha_{A\leftarrow(B),rear}\rangle$	$\frac{3\pi}{4}$ (135°)	$\frac{1}{2}(\sqrt{2}+1)\left[2\left(\sqrt{2}-\frac{5}{4}\right)\pi+1\right]$ (~140.52°)	$\pi - 2/3$ (~141.80°)

Analysis of the Average Configuration-Specific Line-of-Centers Collision Angles. The general expression for any average configuration-specific line-of-centers collision angle for molecule i, $\langle\alpha_{i,k}\rangle$, is

$$\langle\alpha_{i,k}\rangle = \frac{1}{Z_{AB,k}}\int_k \alpha_i\, dZ_{AB}(\alpha_A,\alpha_B,v_A,v_B) \quad (14)$$

in which the integration is over the configuration-specific collision space represented by k (k = front or rear). The expressions for $\langle\alpha_{A,front}\rangle$ and $\langle\alpha_{B,front}\rangle$ are respectively

$$\langle\alpha_{A,front}\rangle = \frac{1}{Z_{AB,front}}\int_0^{\infty}\int_0^{\infty}\int_{\pi/2}^{\pi}\int_0^{\pi/2} \alpha_A\, dZ_{AB}(\alpha_A,\alpha_B,v_A,v_B) = \frac{1}{1+\rho}\left(1+\frac{\pi\rho}{4}\right) \quad (15)$$

$$\langle\alpha_{B,front}\rangle = \frac{1}{Z_{AB,front}}\int_0^\infty\int_0^\infty\int_{\pi/2}^{\pi}\int_0^{\pi/2}\alpha_B\, dZ_{AB}(\alpha_A,\alpha_B,v_A,v_B) = \frac{1}{1+\rho}\left[(\pi-1)\rho+\frac{3\pi}{4}\right] \quad (16)$$

For rear-end collisions, the collision angles are different for the two molecules. There are four distinct angles, and to identify the specific angle, the subscript i in $\langle\alpha_{i,k}\rangle$ is replaced with (i) $\rightarrow j$, $i \rightarrow (j)$, (i) $\leftarrow j$, and $i \leftarrow (j)$, in which the angle is for the molecule in parentheses. The expressions for $\langle\alpha_{(A)\rightarrow B,rear}\rangle$, $\langle\alpha_{A\rightarrow(B),rear}\rangle$, $\langle\alpha_{(A)\leftarrow B,rear}\rangle$, and $\langle\alpha_{A\leftarrow(B),rear}\rangle$ are respectively

$$\langle\alpha_{(A)\rightarrow B,rear}\rangle = \frac{1}{Z_{A\rightarrow B,rear}}\int_0^\infty\int_{\gamma_A}^\infty\int_0^{\pi/2}\int_0^{\pi/2}\alpha_A\, dZ_{AB}(\alpha_A,\alpha_B,v_A,v_B) = \frac{\left(\rho+\frac{1}{\rho}\right)\tan^{-1}(\rho)-1}{2(\sqrt{1+\rho^2}-1)} \quad (17)$$

$$\langle\alpha_{A\rightarrow(B),rear}\rangle = \frac{1}{Z_{A\rightarrow B,rear}}\int_0^\infty\int_{\gamma_A}^\infty\int_0^{\pi/2}\int_0^{\pi/2}\alpha_B\, dZ_{AB}(\alpha_A,\alpha_B,v_A,v_B) = \frac{\left(1+\frac{\pi\rho}{2}\right)\rho-(1+\rho^2)\tan^{-1}(\rho)}{2(\sqrt{1+\rho^2}-1)} \quad (18)$$

$$\langle\alpha_{(A)\leftarrow B,rear}\rangle = \frac{1}{Z_{A\leftarrow B,rear}}\int_{\gamma_B}^\infty\int_0^\infty\int_{\pi/2}^{\pi}\int_{\pi/2}^{\pi}\alpha_A\, dZ_{AB}(\alpha_A,\alpha_B,v_A,v_B)$$

$$\langle\alpha_{(A)\leftarrow B,rear}\rangle = \frac{2\left(\sqrt{1+\rho^2}-\frac{3\rho}{4}\right)\pi-\left(\rho+\frac{1}{\rho}\right)\tan^{-1}(\rho)-1}{2(\sqrt{1+\rho^2}-\rho)} \quad (19)$$

$$\langle\alpha_{A\leftarrow(B),rear}\rangle = \frac{1}{Z_{A\leftarrow B,rear}}\int_{\gamma_B}^\infty\int_0^\infty\int_{\pi/2}^{\pi}\int_{\pi/2}^{\pi}\alpha_B\, dZ_{AB}(\alpha_A,\alpha_B,v_A,v_B)$$

$$\langle\alpha_{A\leftarrow(B),rear}\rangle = \frac{2\left(\sqrt{1+\rho^2}-\frac{1+\rho^2}{4}-\rho\right)\pi+(1+\rho^2)\tan^{-1}(\rho)+\rho}{2(\sqrt{1+\rho^2}-\rho)} \quad (20)$$

Table 2 shows values for all the average configuration-specific line-of-centers collision angles for $\rho = 0$, 1, and ∞. In general, these angles are only weakly dependent upon ρ. Specifically, $\langle\alpha_{A,front}\rangle$ and $\langle\alpha_{B,front}\rangle$ vary by $\sim$12.3° between $\rho = 0$ and $\rho = \infty$, $\langle\alpha_{(A)\rightarrow B,rear}\rangle$ and $\langle\alpha_{A\leftarrow(B),rear}\rangle$ vary by $\sim$6.8°, and $\langle\alpha_{A\rightarrow(B),rear}\rangle$ and $\langle\alpha_{(A)\leftarrow B,rear}\rangle$ vary by $\sim$32.7°.

Analysis of the Average Configuration-Specific Line-of-Centers Speeds. The general expression for the average configuration-specific line-of-centers speed, $\langle v_{lc,k}\rangle$, is

$$\langle v_{lc,k}\rangle = \frac{1}{Z_{AB,k}}\int_k v_{lc}(\alpha_A,\alpha_B,v_A,v_B)\, dZ_{AB}(\alpha_A,\alpha_B,v_A,v_B) \quad (21)$$

The expressions for $\langle v_{lc,front}\rangle$, $\langle v_{lc,A\rightarrow B,rear}\rangle$, and $\langle v_{lc,A\leftarrow B,rear}\rangle$ are respectively

$$\langle v_{lc,front}\rangle = \frac{1}{Z_{AB,front}}\int_0^\infty\int_0^\infty\int_{\pi/2}^{\pi}\int_0^{\pi/2} v_{lc}(\alpha_A,\alpha_B,v_A,v_B)\, dZ_{AB}(\alpha_A,\alpha_B,v_A,v_B)$$

$$\langle v_{lc,front}\rangle = \frac{[4\rho+\pi(1+\rho^2)]\langle v_B\rangle}{4(1+\rho)} \quad (22)$$

$$\langle v_{lc,A\rightarrow B,rear}\rangle = \frac{1}{Z_{A\rightarrow B,rear}}\int_0^\infty\int_{\gamma_A}^\infty\int_0^{\pi/2}\int_0^{\pi/2} v_{lc}(\alpha_A,\alpha_B,v_A,v_B)\, dZ_{AB}(\alpha_A,\alpha_B,v_A,v_B)$$

$$\langle v_{lc,A\rightarrow B,rear}\rangle = \frac{[(1+\rho^2)\tan^{-1}(\rho)-\rho]\langle v_B\rangle}{2(\sqrt{1+\rho^2}-1)} \quad (23)$$

$$\langle v_{lc,A\leftarrow B,rear}\rangle = \frac{1}{Z_{A\leftarrow B,rear}}\int_{\gamma_B}^\infty\int_0^\infty\int_{\pi/2}^{\pi}\int_{\pi/2}^{\pi} v_{lc}(\alpha_A,\alpha_B,v_A,v_B)\, dZ_{AB}(\alpha_A,\alpha_B,v_A,v_B)$$

$$\langle v_{lc,A\leftarrow B,rear}\rangle = \frac{\left\{(1+\rho^2)\left[\frac{\pi}{2}-\tan^{-1}(\rho)\right]-\rho\right\}\langle v_B\rangle}{2(\sqrt{1+\rho^2}-\rho)} \quad (24)$$

Table 3 shows values for the average configuration-specific line-of-centers speeds for $\rho = 0$, 1, and ∞. It bears emphasizing here that the speed at which two colliding molecules impact each other is actually the line-of-centers speed and not the relative speed. The expression for the average relative speed, $\langle v_{rel}\rangle$, is

$$\langle v_{rel}\rangle = \sqrt{\frac{8kT}{\pi\mu}} = \sqrt{1+\rho^2}\langle v_B\rangle \quad (25)$$

On the other hand, the expression for the average line-of-centers speed, $\langle v_{lc}\rangle$, is

$$\langle v_{lc}\rangle = \eta_{front}\langle v_{lc,front}\rangle + \eta_{A\rightarrow B,rear}\langle v_{lc,A\rightarrow B,rear}\rangle + \eta_{A\leftarrow B,rear}\langle v_{lc,A\leftarrow B,rear}\rangle = \frac{\pi}{4}\sqrt{1+\rho^2}\langle v_B\rangle \quad (26)$$

Hence, $\langle v_{lc}\rangle = \pi\langle v_{rel}\rangle/4 \approx 0.7854\langle v_{rel}\rangle$. The expression for $\langle v_{lc}\rangle$, rather than $\langle v_{rel}\rangle$, should be used in analyzing any gas-phase dynamic parameter that is dependent upon the impact speed of two colliding molecules.

Discussion

Outside of pedagogic pursuits and classroom discussions, configuration specificity in gas-phase dynamics has several other potential applications. For one, adding configuration specificity as a higher level of theoretical detail may shed some insight into certain gas-phase dynamic processes such as diffusion and reactivity. For instance, the conventional thought is that molecular collisions always reduce the rate of gaseous diffusion. However, collision events where the diffusing molecules are hit from behind will actually enhance the diffusion rate. Hence, theoretical expressions for the diffusivity are expected to be different if configuration specificity is taken into account. For systems in which classical mechanics applies, configuration specificity may also shed some light in interpreting the results of certain gas-phase experiments such as molecular beam studies. The fact that scattering angles and line-of-centers speeds are different between front- and rear-end collision events may be particularly useful.

TABLE 3: Values for the Average Configuration-Specific Line-of-Centers Speeds for $\rho = 0$, 1, and ∞ ($\rho = \sqrt{m_B/m_A}$ and $\langle v_A \rangle = \rho \langle v_B \rangle$)

	$\rho = 0$	$\rho = 1$	$\rho = \infty$
$\langle v_{lc,front} \rangle$	$\frac{\pi \langle v_B \rangle}{4}$ ($\sim 0.7854 \langle v_B \rangle$)	$\left(1 + \frac{\pi}{2}\right)\frac{\langle v_B \rangle}{2}$ ($\sim 1.285 \langle v_B \rangle$)	$\frac{\pi \langle v_A \rangle}{4}$ ($\sim 0.7854 \langle v_A \rangle$)
$\langle v_{lc,A \rightarrow B,rear} \rangle$	$\frac{2 \langle v_A \rangle}{3}$ ($\sim 0.6667 \langle v_A \rangle$)	$(\sqrt{2} + 1)\left(\frac{\pi}{2} - 1\right)\frac{\langle v_A \rangle}{2}$ ($\sim 0.6890 \langle v_A \rangle$)	$\frac{\pi \langle v_A \rangle}{4}$ ($\sim 0.7854 \langle v_A \rangle$)
$\langle v_{lc,A \leftarrow B,rear} \rangle$	$\frac{\pi \langle v_B \rangle}{4}$ ($\sim 0.7854 \langle v_B \rangle$)	$(\sqrt{2} + 1)\left(\frac{\pi}{2} - 1\right)\frac{\langle v_B \rangle}{2}$ ($\sim 0.6890 \langle v_B \rangle$)	$\frac{2 \langle v_B \rangle}{3}$ ($\sim 0.6667 \langle v_B \rangle$)

It should be emphasized here that, even though configuration specificity does add deeper understanding of gas-phase collision processes, the analysis is limited in its application because of the restrictions that the molecules are spherical and noninteracting. The general results presented in this paper become less applicable for molecules that are structured or exhibit intermolecular interactions. For one, an accurate assessment of the collision cross-section becomes somewhat tenuous for structured molecules. Second, intermolecular potentials will affect the center-of-mass trajectories as well as the internal motion of structured molecules when the molecules are close enough for the force fields to interact. Of course, some of the trends for the nonconfiguration-specific collision parameters in nonideal systems can be predicted with some level of confidence. As a case in point, collision frequencies are expected to be higher for molecules that exhibit attractive interactions. In contrast, even guessing the trends for many of the configuration-specific collision parameters in nonideal systems is difficult without resorting to some level of theoretical analysis.

Acknowledgment. The author graciously thanks Miss Kia Tavares for her expert help in analyzing several of the integrals using Mathematica.

References and Notes

(1) *Kinetic Theory of Gases*; Kauzmann, W., Ed.; W. A. Benjamin, Inc.: New York, 1966.

(2) Wiseman, F. L. *J. Phys. Chem. A* **2006**, *110* (21), 6379.

(3) *Physical Chemistry*; Atkins, A., de Paula, J., Eds.; W. H. Freeman and Company: New York, 2002.

(4) *Mathematica 5.1*; software for technical computation; Wolfram Research: Champaign, IL, 2003: used to perform most of the more complicated integrals and to evaluate some of the limits in Tables 1, 2, and 3.

(5) *Thermodynamics and Kinetics*, 2nd ed.; Benson, S. W., Ed.; Wiley: New York, 1976.

(6) Davis, E. J. *Aerosol Sci. Technol.* **1983**, *2*, 121.